

## Physics-informed Neural Network for Predicting the Moisture Diffusion and Parameter Inversion in Stone Heritage

Jizhong Huang<sup>1,2</sup>, Jinshuai Hu<sup>1,2,3</sup>, Zheng Li<sup>4</sup>, Yue Zhang<sup>1,2</sup>, Yuan Cheng<sup>1,2</sup>

<sup>1</sup> Institute for the Conservation of Cultural Heritage, School of Cultural Heritage and Information Management, Shanghai University, Shanghai, China, 200444 – hjs2022@shu.edu.cn, chengyuan@shu.edu.cn, 2019zhangy@shu.edu.cn, hjizhong@shu.edu.cn

<sup>2</sup> Key Laboratory of Silicate Cultural Relics Conservation (Shanghai University), Ministry of Education – hjs2022@shu.edu.cn, chengyuan@shu.edu.cn, 2019zhangy@shu.edu.cn, hjizhong@shu.edu.cn

<sup>3</sup> School of Mechanics and Engineering Science, Shanghai University, Shanghai, China, 200444 – hjs2022@shu.edu.cn

<sup>4</sup> Department of Cultural Heritage and Museology, Fudan University, Shanghai, 200433, China – zli22@m.fudan.edu.cn

**Keywords:** Stone Heritage, Moisture Diffusion, Physics-informed Neural Network, Data-driven Modeling.

### Abstract

Water vapor is a critical factor affecting the long-term durability of porous stone materials used in historic buildings and archaeological sites. To extend the service life of these materials, it is essential to investigate the mechanisms of water vapor migration within them. This study proposes a multi-domain physics-informed neural network (PINN) framework that integrates physical constraints and data-driven modeling to simulate water vapor diffusion and identify transient diffusion coefficients. The results demonstrate that the PINN model accurately predicts relative humidity distributions in stone samples under both laboratory-controlled and in-situ conditions, achieving mean RMSE values of 1.39 and 3.05, respectively. The inferred diffusion coefficients are consistent with those experimentally determined for Yungang Grotto sandstone, both on the order of  $10^{-7}$ . The PINN framework exhibits improved applicability and computational efficiency. This work presents a robust analytical framework and workflow for characterizing water vapor diffusion behavior and extracting vapor diffusion parameters in porous stone materials.

### 1. Introduction

The preservation of valuable cultural heritage is essential for reinforcing collective identity and promoting social cohesion, while also serving as a foundation for sustainable development in both present and future societies (Ma et al., 2024). However, many immovable heritage sites located in natural environments are subject to ongoing degradation driven by moisture-related processes under hygrothermal conditions. Empirical studies indicate that these deterioration mechanisms are closely associated with complex environmental dynamics, including fluctuations in temperature and humidity, wind-driven rain, water infiltration, capillary rise, and condensation. Sustained high humidity and water ingress facilitate microbial growth, leading to fungal and moss colonization on mural surfaces. Cyclic hygrothermal stresses caused by alternating temperature and humidity accelerate granular exfoliation of stone surfaces (Hu et al., 2024). The combined effects of these physical, chemical, and biological processes can ultimately lead to the irreversible loss of culturally significant surface features. Given that vapor diffusion is a key mechanism of moisture transport in humid environments, a comprehensive understanding of vapor transport dynamics is essential (Zhang et al., 2022). Investigating moisture diffusion mechanisms provides a scientific basis for developing sustainable conservation practices.

The determination of parameters for both steady-state and transient vapor diffusion models primarily depends on laboratory experiments (e.g., wet-dry cup tests) and field monitoring (e.g., hygrothermal sensors). However, these approaches are often prohibitively time-consuming (Zhang et al., 2022). Although numerical simulations serve as valuable alternatives, their predictions frequently deviate from experimental results due to inherent model approximations, uncertainties in boundary and initial conditions, inaccuracies in parameterization, and computational limitations (Hu et al., 2024). Moreover, the spatiotemporal variability of moisture

distribution within porous stone driven by complex environmental interactions necessitates high-resolution physical parameter measurements, which are not adequately captured by conventional laboratory testing under controlled conditions. While environmental monitoring remains a key component of heritage conservation, current practices typically restricted to non-invasive or minimally intrusive techniques primarily target ambient temperature and humidity. These methods fail to resolve critical subsurface processes such as internal moisture content fluctuations, condensation-evaporation cycles, and thermally driven vapor transport (Qaddah et al., 2023). The inability to quantify essential parameters, such as moisture diffusion coefficients, hampers the development of accurate, long-term preventive conservation strategies based on mechanistic models of moisture transport.

Machine learning presents promising opportunities for elucidating moisture diffusion mechanisms and developing surrogate models based on long-term dynamic environmental monitoring data, while simultaneously capturing transient vapor transport behavior. However, data-driven models are inherently limited by their black-box nature, which poses challenges such as data incompleteness, measurement noise, suboptimal training procedures, and risks of underfitting or overfitting. Moreover, these models lack physical interpretability, as they are constructed independently of fundamental conservation laws. To overcome these limitations while leveraging the complementary strengths of data-driven and physics-based approaches, physics-informed neural networks (PINNs) have emerged as a transformative modeling framework (Wang et al., 2023). Physics-informed neural networks (PINNs) enhance model interpretability by incorporating governing partial differential equations (PDEs) directly into the neural network architecture. These models are trained by minimizing a composite loss function that enforces two constraints: consistency with physical laws through PDE residuals and agreement with empirical data. This hybrid approach also facilitates inverse parameter estimation by enabling the

identification of vapor diffusion coefficients from indirect environmental monitoring data, thereby overcoming the limitations of direct measurement techniques in heritage conservation applications.

This study introduces a novel physics-informed data-driven framework to establish surrogate models for moisture diffusion in sandstone heritage artifacts, enabling concurrent resolution of forward (relative humidity prediction) and inverse (diffusion coefficient estimation) problems. The methodology initiates with laboratory-based monitoring of vapor diffusion dynamics using a custom-designed apparatus comprising calibrated relative humidity sensors, a signal acquisition module, an environmental chamber, and a data-logging platform. Cylindrical sandstone samples from the Yungang Grottoes (120 mm edge-length cubes, epoxy-sealed on four surfaces with two opposing diffusion interfaces) were instrumented to record humidity variations at five depth intervals (20, 40, 60, 80, and 100 mm from the diffusion surface), generating experimental datasets for training deep neural networks. A Physics-Informed Neural Network (PINN) architecture was developed by integrating Fick's second law through a dual residual formulation simultaneously minimizing data-driven prediction errors and physical law violations. This hybrid loss function ensures consistency with fundamental diffusion principles while solving the governing PDE numerically. The model's key innovation lies in its dual-problem resolution capability, where spatiotemporal features are processed to simultaneously predict humidity distributions (forward problem) and infer moisture diffusion coefficients (inverse problem), effectively bridging theoretical predictions with empirical observations.

Subsequent sections are organized as follows: Section 2 details the mathematical framework for forward modeling of humidity distributions and the implementation of the physics-constrained deep learning architecture for inverse parameter identification. Section 3 presents quantitative validation of the PINN's predictive accuracy, discusses performance metrics, and evaluates the model's generalization capacity. Finally, Section 4 concludes with methodological implications, proposes refinements for multi-physics coupling scenarios, and outlines future applications of physics-guided machine learning paradigms in hygrothermal conservation science.

## 2. Data Acquisition

The Yungang Grottoes, recognized as the earliest Buddhist cave temple complex commissioned by imperial authority in China and a masterpiece of global Buddhist rock-cut architecture, were inscribed as a UNESCO World Heritage Site in 2001. Sandstone specimens used in the laboratory experiments were collected from the rear hills of the Yungang Grottoes, specifically from fresh rock strata corresponding to the same stratigraphic layer as the stone carvings within the caves. Sampling was conducted at depths of no less than 20 cm below the surface to ensure material consistency and minimize weathering effects. The sandstone in the Yungang Grottoes is characterized as a porous medium with interconnected channel structures that facilitate water vapor diffusion. The complex microclimatic conditions within the grottoes, combined with recurring freeze–thaw cycles, have progressively contributed to the weathering of these invaluable stone carvings, with surface deterioration manifesting as exfoliation, detachment, and other forms of material loss. Accordingly, freeze–thaw cycle experiments were conducted on sandstone specimens, and ultrasonic pulse velocity measurements were employed to evaluate the extent of weathering.

The sandstone was cut into cubic specimens with dimensions of  $120 \times 120 \times 120 \text{ mm}^3$  using a rock-cutting machine. Five holes, each 7 mm in diameter and 60 mm in depth, were drilled along the central axis of each specimen at 20 mm intervals, corresponding to depths of 20, 40, 60, 80, and 100 mm from the diffusion surface, to accommodate humidity sensors under controlled environmental conditions (relative humidity: 80%; temperature:  $15^\circ\text{C}$ ).

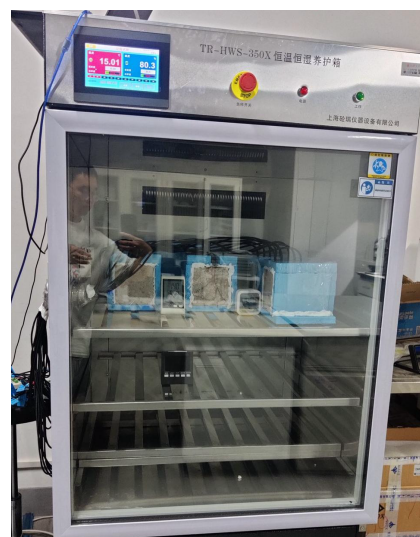


Figure 1. Moisture diffusion Monitoring System for Sandstone Heritage.

## 3. Methodology

Previous researchers have derived physical laws through experimental observation and theoretical deduction. However, experimental data often implicitly contains inherent physical relationships. When dealing with large-scale datasets, machine learning methods provide an efficient and economical approach to building surrogate models. However, traditional machine learning methods generally lack physical interpretability. Therefore, it is necessary to combine existing physical laws with neural network approaches by incorporating physical laws as constraint conditions for unknown functions, guiding the neural network to converge towards surrogate models that have physical interpretability. This section begins by presenting the partial differential equations (PDEs) that govern the fundamental physical principles of water vapor diffusion. These equations are subsequently embedded as physical constraints within the data-driven neural network framework. The following subsections detail the architecture of the neural network and the implementation strategy for incorporating the physical constraints.

### 3.1 Governing Equation

This transport behavior follows Fick's law of diffusion, which theoretically characterizes the mass transfer of moisture in porous media under the combined influence of concentration gradients and the diffusion coefficient (Cuomo et al., 2022).

$$\frac{\partial C}{\partial t} = D \cdot x \cdot t \cdot \frac{\partial^2 C}{\partial x^2} \quad (1)$$

Where  $t$  represents the diffusion time of water vapor in seconds,  $D(x, t)$  is the nonlinear diffusion coefficient, a function of depth and time, measured in  $\text{mm}^2/\text{s}$ . Here,  $x$  is the depth within the rock in mm, and  $C$  is the water vapor concentration in  $\text{mol}/\text{m}^3$ .

### 3.2 Physics-informed Neural Networks Model

In previous studies, deep neural networks (DNNs) were primarily employed as purely data-driven approaches to approximate the physical process. However, these models depend solely on empirical training data and are devoid of constraints imposed by underlying physical principles (Goswami et al., 2020). While DNNs may achieve high predictive accuracy when trained on large, high-quality datasets, their performance typically deteriorates in data-limited scenarios (Li et al., 2024). To improve adherence to physical laws, the present study incorporates partial differential equation (PDE) constraints into the model's loss function, thereby embedding governing physical principles directly into the learning process. The subsequent sections provide a detailed description of the implementation strategy adopted for the physics-informed neural network (PINN) framework.

This section introduces the Physics-Informed Neural Network (PINN) framework developed to simulate water vapor diffusion behavior in porous rock materials. The framework integrates physical laws into a data-driven neural network surrogate model, ensuring that the predicted results are not only consistent with observed data but also adhere to the governing physical principles of vapor diffusion. Furthermore, the PINN framework facilitates the identification of diffusion parameters from indirect measurements.

Figure 2 illustrates the architecture of the PINN model employed to estimate water vapor diffusion behavior in sandstone. A defining feature of the framework is its explicit incorporation of physical constraints into a conventional deep neural network structure. The network comprises an input layer, multiple hidden layers with residual connections, fully connected layers, and an output layer (Hornik et al., 1989). This mapping relationship can be formally expressed as:

$$C \cdot x \cdot t = N \cdot x \cdot t \cdot w \cdot b = N \cdot x \cdot t \cdot \theta \quad (2)$$

Where  $N$  is the neural network mapping, and  $\theta$  denotes the trainable parameters of the network, including weights  $w$  and biases  $b$ . The network optimizes its parameters  $\theta$  using the backpropagation algorithm to minimize the loss function, typically quantified by the mean squared error (MSE) between predicted and observed values (Cuomo et al., 2022).

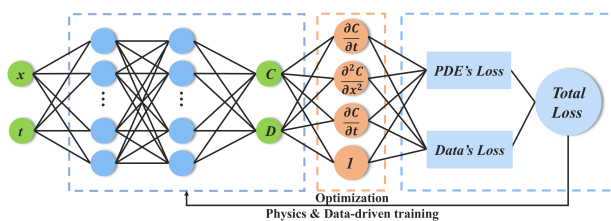


Figure 2. Hybrid Physics-Informed and Data-Driven Neural Network Framework

The proposed model integrates finite difference schemes with physics-informed neural networks (PINNs). Specifically, a forward difference scheme is applied for temporal derivatives, while a central difference scheme is utilized for spatial derivatives (Abdar et al., 2021). Simultaneously, automatic differentiation is employed to compute the gradients of the total loss with respect to neural network parameters, facilitating efficient optimization during training.

The loss function of the physics-informed neural network (PINN) comprises multiple components. The data loss term,  $L_{Data}$ , measures the discrepancy between the model's predictions and the observed experimental data. In addition, physical constraints derived from the governing diffusion equation are incorporated as regularization terms, forming the physical loss component,  $L_{Eqn}$ , which quantifies the deviation between the model-estimated diffusion behaviour and the expected physical behavior. A boundary condition loss term,  $L_{BC}$ , is also included to enforce compliance with prescribed boundary conditions. The physical loss term employs the Huber loss function, proposed by the statistician Peter Huber ("Robust learning of Huber loss under weak conditional moment," 2022).

$$L_{total} = \lambda_{data} L_{data} + \lambda_{Eqn} L_{Eqn} + \lambda_{BC} L_{BC} \quad (3)$$

$\lambda_{data}$  and  $\lambda_{Eqn}$  represent the weighting coefficients for the data loss and physical constraint loss, respectively. These coefficients are optimized via hyperparameter tuning during the initial phase of training. The network weights and biases are iteratively updated using the AdamW optimization algorithm to minimize the total loss and obtain the optimal network parameters  $\theta^*$  (Lu et al., 2021; Raissi et al., 2019; Wang et al., 2024).

$$\theta^* = \dots \cdot L \cdot \theta \quad (4)$$

In this study, The diffusion coefficient is modeled as a nonlinear function of both space and time, denoted as  $D(x,t)$ , rather than assumed to be spatially and temporally constant. Hyperparameter tuning is conducted using Bayesian optimization implemented via Optuna's Tree-structured Parzen Estimator (TPE) sampler ("Optuna | Proceedings of the 25th ACM SIGKDD International Conference on Knowledge Discovery & Data Mining," n.d.). This dynamic adjustment helps the optimizer escape local minima and promotes better generalization performance (Raissi et al., 2019). Upon completion of training, the PINN model's predictions are quantitatively compared with experimental observations to assess its ability to accurately reproduce real-world water vapor diffusion behavior in porous materials

### 3.3 Model Evaluation

To evaluate the model's performance in capturing the dynamics of water vapor diffusion in porous stone materials, two cross-validation strategies are employed during training: depth-wise cross-validation and temporal window cross-validation. These strategies are specifically designed to assess the spatiotemporal generalization capabilities of the physics-informed neural network (PINN) model. The depth-wise cross-validation approach follows a leave-one-depth-out scheme, where each spatial layer (i.e., measurement depth) is sequentially held out as the test set while the remaining depths are used for training. This setup evaluates the model's ability to generalize across different spatial positions within the material. The temporal window cross-validation divides the data into overlapping time intervals using a sliding window mechanism. At each step, a portion of the time-series data is reserved for validation, allowing assessment of the model's performance across time and its extrapolation capability beyond the training horizon.

Model accuracy is quantitatively assessed using three standard error metrics: Mean Absolute Error (MAE), Mean Squared Error (MSE), and Root Mean Squared Error (RMSE) (Waheed et al., 2021). These metrics provide complementary insights into prediction accuracy and robustness. Lower values of MAE, MSE, and RMSE indicate superior predictive performance and

better alignment between the model outputs and experimental measurements.

$$MAE = \frac{1}{n} \sum_{i=1}^n |y_i - \hat{y}_i| \quad (9)$$

$$RMSE = \sqrt{\frac{1}{n} \sum_{i=1}^n (y_i - \hat{y}_i)^2} \quad (10)$$

$$MSE = \frac{1}{n} \sum_{i=1}^n (y_i - \hat{y}_i)^2 \quad (11)$$

$y_i$  denotes the observed value,  $\hat{y}_i$  the corresponding predicted value, and  $n$  the number of data points.

#### 4. Results and Discussion

In this section, a physics-informed and data-driven PINN framework is utilized to simulate water vapor diffusion behavior in rock samples collected from laboratory experiments. The model simultaneously predicts the spatiotemporal distribution of vapor concentration and estimates the corresponding non-stationary diffusion coefficient, thereby capturing the dynamic transport characteristics of porous stone materials under varying environmental conditions.

##### 4.1 Results of PINN in Forward Problem and Parameter Identification

As illustrated in Figure 3, fluctuations in ambient relative humidity initiate a quasi-one-dimensional vapor diffusion process within the rock matrix, resulting in the formation of a humidity gradient across the 20 mm to 100 mm depth range. The sharp increase in relative humidity observed during the initial stages is primarily attributed to the definition of relative humidity as the ratio of vapor pressure to saturation pressure. Under this formulation, a steeper water concentration gradient yields a larger vapor pressure differential, which in turn accelerates the diffusion process. With increasing depth, both the magnitude of the humidity gradient and its temporal rate of change progressively diminish. As vapor diffusion continues, the relative humidity profiles gradually level off, and the inter-point gradients decrease, reflecting a reduction in transport intensity.

Following the training phase, the PINN model is employed to predict the spatiotemporal distribution of relative humidity across various depths, as illustrated in Figure 3(f). The results demonstrate that the model successfully captures the essential characteristics of water vapor diffusion within the sandstone medium and enables reliable prediction of relative humidity at arbitrary locations within the defined spatial-temporal domain. The predicted values exhibit strong agreement with experimental measurements across five monitoring depths (20 mm, 40 mm, 60 mm, 80 mm, and 100 mm), with corresponding average RMSE values of approximately 1.90, 1.15, 0.90, 0.97, and 2.01, respectively. Among these, the prediction at the 60 mm depth achieves the highest accuracy, which is likely attributable to the relatively stable humidity profile at this depth—resulting in lower modeling complexity and reduced prediction error. Although the model exhibits slightly reduced performance at the 20 mm depth, primarily due to more pronounced and transient humidity fluctuations near the surface, it still maintains a high level of predictive accuracy. These findings underscore the model's robustness and effectiveness in capturing complex vapor transport behaviors in porous stone materials.

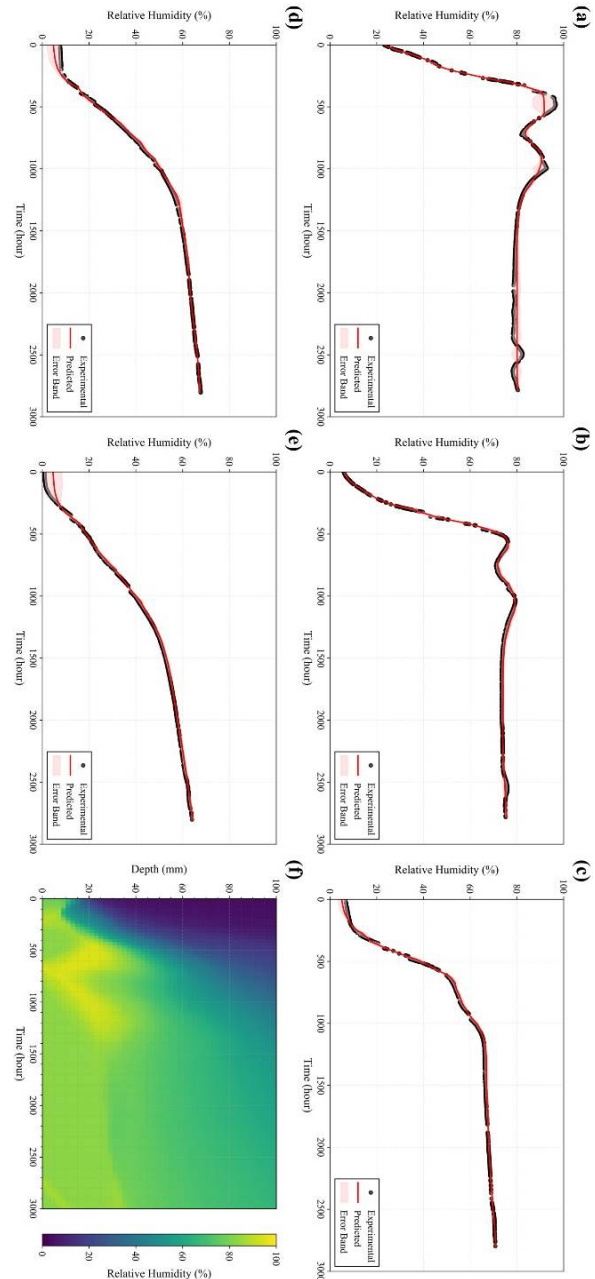


Figure 3. Comparison between PINN predictions and measured data in laboratory; (a) 20mm; (b) 40mm; (c) 60mm; (d) 80mm; (e) 100mm; (f) Heatmap of predicted RH in Sandstone

To achieve a more accurate quantification of water vapor diffusion rates, the PINN framework is designed to simultaneously infer the spatial-temporal distribution of the water vapor diffusion coefficient during the training process. As illustrated in Figure 4, the model successfully estimates the transient diffusion coefficients at multiple depths within the sandstone medium. This inversion process is particularly critical because the physical parameters that govern vapor diffusion—especially at internal and boundary locations—are typically unmeasurable through direct experimental methods and may exhibit substantial spatial or temporal variability. Therefore, incorporating parameter inference within the PINN training not only enhances model fidelity but also provides valuable insight into the underlying transport mechanisms. Previous studies have



reported that the water vapor diffusion coefficient in Yungang Grotto sandstone ranges from  $2.16 \times 10^{-7} \text{ m}^2/\text{s}$  to  $13.99 \times 10^{-7} \text{ m}^2/\text{s}$  (Zhang et al., 2022), which is consistent in order of magnitude with the inferred values obtained from our model (approximately  $10^{-7} \text{ m}^2/\text{s}$ ). This agreement not only validates the accuracy of the PINN-based inversion but also underscores its reliability in characterizing vapor transport properties in porous sandstone materials.

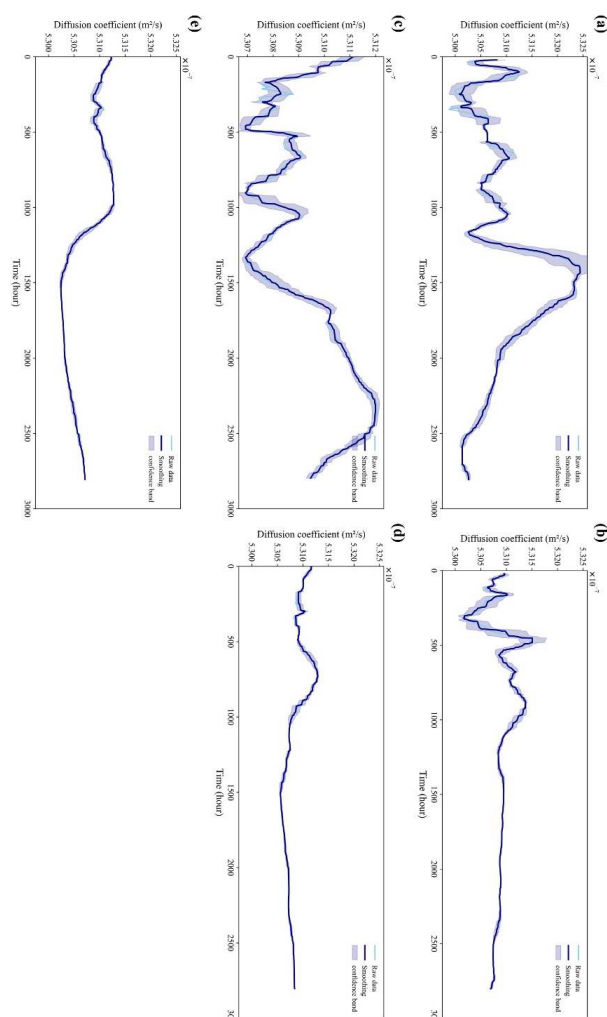


Figure 4. Water vapor diffusion coefficient identification using PINN in laboratory; (a) 20mm; (b) 40mm; (c) 60mm; (d) 80mm; (e) 100mm.

Although slight deviations are observed between the inferred and theoretical values, these discrepancies may be attributed to several factors, including limited boundary condition data, sparse humidity measurements, and inherent uncertainties in estimating spatially heterogeneous diffusion coefficients. To enhance the accuracy of PINN-based parameter inversion, additional high-resolution experimental data are required to better capture spatial variability and reduce estimation bias (Wang et al., 2021).

## 4.2 Accuracy

To further validate the effectiveness and superiority of the proposed PINN model in simulating water vapor diffusion within porous stone materials. The performance of PINN summarized in Table 1. As Table 1 illustrated, the PDNN model achieves lower RMSE, MAE, and MSE values on laboratory

datasets. The PINN model demonstrates robust performance in predicting internal relative humidity distributions within porous stone under controlled laboratory conditions. Laboratory experiments yielded average RMSE values for relative humidity predictions at depths of 20 mm, 40 mm, 60 mm, 80 mm, and 100 mm of approximately 1.90, 1.15, 0.90, 0.97, and 2.01, respectively.

Table 1 Performance of PINN.

| Models | Depth(mm) | RMSE | MSE  | MAE  |
|--------|-----------|------|------|------|
| PINN   | 20        | 1.90 | 5.01 | 1.35 |
|        | 40        | 1.15 | 2.21 | 0.90 |
|        | 60        | 0.90 | 1.31 | 0.67 |
|        | 80        | 0.97 | 1.27 | 0.68 |
|        | 100       | 2.01 | 6.22 | 1.39 |

## 5. Conclusion

This study presents a physics-informed and data-driven hybrid framework, referred to as PINN, designed to predict internal relative humidity distributions and infer water vapor diffusion coefficients within porous stone materials. By embedding the diffusion equation as an explicit physical constraint, the PINN framework effectively integrates fundamental physical laws with observational data. This integration enables the accurate reproduction of water vapor transport dynamics in porous stone and facilitates the quantitative estimation of diffusion coefficients that vary across spatial and temporal dimensions. The key conclusions derived from this work are summarized as follows:

- (1) The PINN model demonstrates robust performance in predicting internal relative humidity distributions within porous stone under controlled laboratory conditions. Laboratory experiments yielded average RMSE values for relative humidity predictions at depths of 20 mm, 40 mm, 60 mm, 80 mm, and 100 mm of approximately 1.90, 1.15, 0.90, 0.97, and 2.01, respectively. These results validate the model's capability to serve as an efficient and reliable tool for real-time prediction of moisture diffusion processes in porous stone materials.
- (2) The PINN model successfully identifies spatiotemporally dependent, non-stationary water vapor diffusion coefficients. The inferred coefficients are on the order of magnitude of approximately  $10^{-7} \text{ m}^2/\text{s}$ , consistent with experimentally measured values reported for sandstone from the Yungang Grottoes. These results demonstrate the model's accuracy and effectiveness in capturing the moisture transport characteristics of porous materials in cultural heritage contexts.

## Acknowledgements

This research was supported by Scientific and Technological Research Project of Cultural Relics of State Administration of Cultural Heritage (No. 2023ZCK014), Project of Key Laboratory of Silicate Cultural Relics Conservation (Shanghai University), Ministry of Education (No. SCRC2024KF06YQ, SCRC2024ZZ02ZD), Science and Technology Major Special Program Project of Shanxi Province (No. 202201150501024) and the Tencent Tanyuan Program 2024. The authors thank Yungang Research Institute for providing assistance and

support with data acquisition, and Shanghai Technical Service Center of Science and Engineering Computing at Shanghai University for computational resources.

## References

- Abdar, M., Pourpanah, F., Hussain, S., Rezazadegan, D., Liu, L., Ghavamzadeh, M., Fieguth, P., Cao, X., Khosravi, A., Acharya, U.R., Makarek, V., Nahavandi, S., 2021. A review of uncertainty quantification in deep learning: Techniques, applications and challenges. *Inf. Fusion* 76, 243–297.
- Cuomo, S., Di Cola, V.S., Giampaolo, F., Rozza, G., Raissi, M., Piccialli, F., 2022. Scientific Machine Learning Through Physics-Informed Neural Networks: Where we are and What's Next. *J. Sci. Comput.* 92, 88.
- Goswami, S., Anitescu, C., Chakraborty, S., Rabczuk, T., 2020. Transfer learning enhanced physics informed neural network for phase-field modeling of fracture. *Theor. Appl. Fract. Mech.* 106, 102447.
- Hornik, K., Stinchcombe, M., White, H., 1989. Multilayer feedforward networks are universal approximators. *Neural Netw.* 2, 359–366.
- Hu, J., Cheng, Y., Li, Z., Huang, J., Zhang, Y., Yan, H., n.d. Research on the Anisotropy of the Thermal Conductivity of Sandstone Heritage via Digital Rock Physics Under Various Pore Media. *Int. J. Archit. Herit.* 0, 1–17.
- Hu, J., Huang, J., Cheng, Y., 2024. Experimental study evaluating the performance of thermal conductivity prediction models for air–water saturated weathered sandstone heritage. *Herit. Sci.* 12, 366.
- Li, K.-Q., Yin, Z.-Y., Zhang, N., Li, J., 2024. A PINN-based modelling approach for hydromechanical behaviour of unsaturated expansive soils. *Comput. Geotech.* 169, 106174.
- Lu, L., Meng, X., Mao, Z., Karniadakis, G.E., 2021. DeepXDE: A deep learning library for solving differential equations. *SIAM Rev.* 63, 208–228.
- Ma, Y., Xie, H., Li, Y., Hokoi, S., Zhang, X., Wang, X., 2024. Water-related deterioration risk assessment for sustainable conservation of heritage buildings in the Forbidden City, China. *Dev. Built Environ.* 17, 100293.
- Optuna | Proceedings of the 25th ACM SIGKDD International Conference on Knowledge Discovery & Data Mining [WWW Document], n.d. *ACM Conf.*
- Qaddah, B., Soucasse, L., Doumenc, F., Mergui, S., Rivière, Ph., Soufiani, A., 2023. Coupled heat and mass transfer in shallow caves: Interactions between turbulent convection, gas radiative transfer and moisture transport. *Int. J. Therm. Sci.* 194, 108556.
- Raissi, M., Perdikaris, P., Karniadakis, G.E., 2019. Physics-informed neural networks: A deep learning framework for solving forward and inverse problems involving nonlinear partial differential equations. *J. Comput. Phys.* 378, 686–707.
- Robust learning of Huber loss under weak conditional moment, 2022. *Neurocomputing* 507, 191–198.
- Waheed, U. bin, Haghighat, E., Alkhalifah, T., Song, C., Hao, Q., 2021. PINNeik: Eikonal solution using physics-informed neural networks. *Comput. Geosci.* 155, 104833.
- Wang, N., Chang, H., Zhang, D., 2021. Deep-Learning-Based Inverse Modeling Approaches: A Subsurface Flow Example. *J. Geophys. Res. Solid Earth* 126, e2020JB020549.
- Wang, Y., Shi, L., Hu, X., Song, W., Wang, L., 2023. Multiphysics-informed neural networks for coupled soil hydrothermal modeling. *Water Resour. Res.* 59, e2022WR031960.
- Wang, Y., Yao, Y., Guo, J., Gao, Z., 2024. A practical PINN framework for multi-scale problems with multi-magnitude loss terms. *J. Comput. Phys.* 510, 113112.
- Zhang, Y., Zheng, Y., Huang, J., 2022. Determination of Water Vapor Transmission Properties of Sandstones in the Yungang Grottoes. *Int. J. Archit. Herit.* 0, 1–13.